Effect of Material Gradient on Stresses of FGM Rotating Thick-Walled Cylindrical Pressure Vessel with Longitudinal Variation of Properties under Non-Uniform Internal and External Pressure

Mehdi Jabbari[1], Mohammad Zamani Nejad[1,6], Mehdi Ghannad[2]

[1]*Mechanical Engineering Department, Yasouj University, P.O. Box: 75914-353, Yasouj, Iran*
[2]*Mechanical Engineering Faculty, Shahrood University, Shahrood, Iran*

ARTICLE INFO

Article history:

Received 9 September 2015
Accepted 2 July 2016
Available online 15 July 2016

Keywords:

Thick cylindrical shell
Functionally graded material (FGM)
Multi-layered method (MLM)
Longitudinal variation of properties
Non-uniform pressure

ABSTRACT

The present paper provides a semi-analytical solution to obtain the displacements and stresses in a functionally graded material (FGM) rotating thick cylindrical shell with clamped ends under non-uniform pressure. Material properties of cylinder are assumed to change along the axial direction according to a power law form. It is also assumed that the Poisson's ratio is constant. Given the existence of shear stress in the thick cylindrical shell due to material and pressure changes along the axial direction, the governing equations are obtained based on first-order shear deformation theory (FSDT). These equations are in the form of a set of general differential equations with variable coefficients. Given that the FG cylinder is divided into n homogenous disks, n sets of differential equations with constant coefficients are obtained. The solution of this set of equations, applying the boundary conditions and continuity conditions between the layers, yields displacements and stresses. The problem was also solved, using the finite element method (FEM), the results of which were compared with those of the multi-layered method (MLM). Finally, some numerical results are presented to study the effects of applied pressure, non-homogeneity index, and power law index of FGM on the mechanical behavior of the cylindrical shell.

1. Introduction

Functionally graded materials (FGMs) are advanced composite materials whose mechanical properties vary continuously from one surface to another at macro level[1]. They are now developed for general use as structural components in extremely high-temperature environments. The ability to predict the response of FGM shells when subjected to thermal and mechanical loads is of prime interest to structural analysis[2-5].

Elastic analysis of FGM thick-walled cylindrical shells has been intensively investigated in the literature. Lame[6] studied the exact solution of a thick homogenous and isotropic cylinder under inner and outer pressures. Assuming the cross shear effect,Naghdi and Cooper[7] formulated the shear deformation theory (SDT). Mirsky and Hermann [8] derived the solution of thick cylindrical shells of homogenous and isotropic materials by using the first shear deformation theory (FSDT). The plane strain and anti-plane shear problems for the general multi-layered composites were considered by Erdogan and Gupta [9]. Shirakawa [10] studied the effect of shear deformation on the displacements and

∗ Corresponding author:
E-mail: m.zamani.n@gmail.com; m_zamani@yu.ac.ir

stresses in a cylindrical shell under a static load. Reddy [11] presented a higher-order shear deformation theory of plates accounting for the von Karman strains. This theory contains the same dependent unknowns as the Hencky-Mindlin type FSDT and accounts for parabolic distribution of the transverse shear strains through the thickness of the plate. Horgan and Chan[12] investigated the effects of material inhomogeneity on the response of linearly elastic isotropic hollow circular cylinders or disks under uniform internal or external pressure. Niordson[13] derived the two-dimensional shell equations for a circular cylindrical shell by means of an asymptotic expansion of the three-dimensional elastic state.

Using a profile for the volume fraction and a normal-mode expansion of motion equations yields a system of Mathieu-Hill equations, Ng et al.[14] presented a formulation for the dynamic stability analysis of functionally graded shells under harmonic axial loading by the Bolotin's method. Pan and Roy[15] derived exact solutions for multilayered FGM cylinders under static deformation. They obtained these solutions by separation of variables and expressed it in terms of the summation of the Fourier series in the circumferential direction. Xiang et al. [16] provided the elastic analysis and exact solution for stresses in FGM hollow cylinders in the state of plane strain with isotropic multi-layers based on Lamé's solution. Kang [17] derived the field equations for homogenous thick shells of revolution.

A complete and consistent 3-D set of field equations was developed by tensor analysis to characterize the behavior of FGM thick shells of revolution with arbitrary curvature and variable thickness along the meridional direction by Zamani Nejad et al. [18]. Using the 3D linear elastic theory, Santos et al. [19] developed a study of free vibrations of FGM shells made up of isotropic properties by a semi-analytical axisymmetric finite element model. Using plane elasticity theory and Complementary Functions method, Tutuncu and Temel [20] obtained axisymmetric displacements and stresses in FG hollow cylinders, disks, and spheres subjected to uniform internal pressure. Zamani Nejad and Rahimi [21] obtained stresses in isotropic rotating FGM thick-walled cylindrical pressure vessels as a function of radial direction by using the theory of elasticity. Arani et al. [22] investigated thermo-piezo-magnetic behavior of an FG piezo-magnetic rotating disk under mechanical and thermal loads. They expressed power functions in radial direction of the disk by using mathematical modeling. Assuming that the Young's modulus varies nonlinearly in the radial direction, and that the Poisson's ratio is constant, on the basis of plane elasticity theory, Ghannad and Zamani Nejad [23] derived the governing equations for axisymmetric thick cylindrical shells made of nonhomogeneous FGMs subjected to internal and external pressure. A high-order theory for FG axially symmetric cylindrical shell based on the expansion of the axially symmetric equations of elasticity was developed by Zozulya [24] for functionally graded materials into Legendre polynomials series. Making use of FSDT, Ghannad and Zamani Nejad obtained displacements and stresses of internally pressurized clamped-clamped thick isotropic axisymmetric homogeneous [25] and FGMs [26] cylinders. Ghannad and Gharooni [27] presented an elastic analysis and a closed form analytical solution for rotating FG thick walled hollow cylindrical shells subjected to constant internal and/or external pressure. Assuming that the modulus of elasticity varies in the radial direction as power function, Khoshgoftar et al. [28] presented an elastic solution for thick-walled cylindrical pressure vessels under longitudinally non-uniform pressure made of FG materials. Ghannad et al. obtained an analytical solution for stresses and radial displacement of homogeneous [29] and FGM [30] clamped-clamped pressurized thick cylindrical shells with variable thickness using FSDT and matched asymptotic method. Asemi et al. [31] studied a thick truncated hollow cone with a finite length made of two dimensional functionally graded materials subjected to combined loads. The volume fraction distribution of materials and geometry were assumed to be axisymmetric but not uniform along the axial direction. Using disk form multilayers, Zamani Nejad et al. [32] derived a semi-analytical solution for the purpose of determining displacements and stresses in a rotating cylindrical shell with variable thickness under uniform pressure. Arani et al. [33] studied static stresses analysis of carbon nano-tube

reinforced composite cylinder made of poly-vinylidene fluoride subjected to non-axisymmetric thermomechanical loads. Batra [34] obtained direct and material tailoring (or inverse) problems for finite torsional deformations of a solid circular cylinder made of a Mooney–Rivlin material with the two elastic moduli continuously varying in the axial direction and deformed by applying equal and opposite torques on its two end faces. Zamani Nejad et al. [35] derived a semi-analytical solution for determination of displacements and stresses in a thick cylindrical shell with variable thickness under non-uniform pressure. They considered three different profiles (convex, linear and concave) for the variable thickness cylinder. Shariati et al. [36] presented a numerical analysis of stresses and displacements in FGM thick-walled cylindrical pressure vessel under internal pressure. They assumed the elastic modulus varying along the longitude of the pressure vessel with an exponential function continuously.

As mentioned above, numerous studies have been carried out on cylinders made of functionally graded material with radial-directionally dependent properties. In the present study, taking into account the effect of shear stresses and strains, the FSDT of derivation and elastic analysis of a non-uniform pressurized thick-walled cylinder shell made of axially functionally graded material with clamped-clamped ends are presented. Using multi-layered method (MLM), an FGM rotating cylindrical shell with axially-varying properties is divided into *n* homogenous disks. With regard to the continuity between layers and applying boundary conditions, the governing set of differential equations with constant coefficients is solved. The results obtained for stresses and displacements are compared with the solutions obtained by the finite element method (FEM). Good agreement was found between the results.

2. Problem Formulation

In SDT, the straight lines perpendicular to the central axis of the cylinder do not necessarily remain unchanged after loading and deformation, suggesting that the deformations are axially axisymmetric and change along the longitudinal cylinder. In other words, the elements have rotation and the shear strain is not zero. Consider a clamped-clamped thick-walled isotropic FGM cylinder with an inner radius r_i, thickness h, and length L subjected to internal pressures $P_{in}(x)$ and external pressure $P_{out}(x)$. The cylinder is rotating around its axis with constant angular velocity μ (Fig. 1)

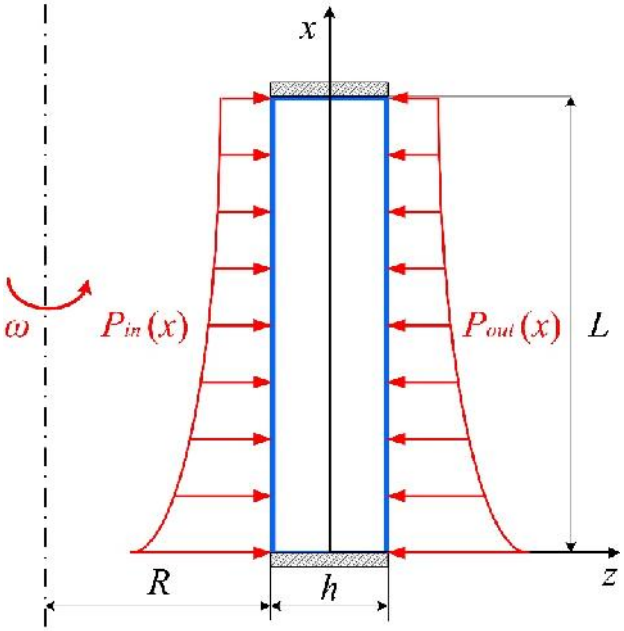

Fig 1. Cross section of the thick rotating cylinder with clamped-clamped ends

The location of any typical point within the shell element may be determined by R and z is as follows:

$$r = R + z \tag{1}$$

where R represents the distance of the middle surface from the axial direction and z is the distance of any typical point from the middle surface. With respect to Fig. 1, x and z must be as follows:

$$\begin{cases} -\dfrac{h}{2} \le z \le \dfrac{h}{2} \\ 0 \le x \le L \end{cases} \tag{2}$$

where h and L are the thickness and the length of the cylinder, respectively. The general axisymmetric displacement field, (U_x, U_z), in the FSDT could be expressed on the basis of axial and radial displacements as follows:

$$\begin{Bmatrix} U_x \\ U_z \end{Bmatrix} = \begin{Bmatrix} u(x) \\ w(x) \end{Bmatrix} + \begin{Bmatrix} ¤(x) \\ \cdot(x) \end{Bmatrix} z \tag{3}$$

where $u(x)$ and $w(x)$ are the displacement components of the middle surface, respectively. Also, $¤(x)$ and $\cdot(x)$ are the functions of displacement field. The strain-displacement relations in the cylindrical coordinates system are:

$$\begin{cases} £_x = \dfrac{\partial U_x}{\partial x} = \dfrac{du}{dx} + \dfrac{d¤}{dx} z \\ £_{-} = \dfrac{U_z}{r} = \dfrac{1}{R+z}(w + \cdot z) \\ £_z = \dfrac{\partial U_z}{\partial z} = \cdot \\ ¥_{xz} = \dfrac{\partial U_x}{\partial z} + \dfrac{\partial U_z}{\partial x} = \left(¤ + \dfrac{dw}{dx}\right) + \dfrac{d\cdot}{dx} z \end{cases} \tag{4}$$

Material properties including the modulus of elasticity E and density $°$ are supposed to be axially dependent and are assumed to vary as follows:

$$E = E_1 + (E_2 - E_1)\left(\frac{x}{L}\right)^{n_1} \tag{5a}$$

$$° = °_1 + (°_2 - °_1)\left(\frac{x}{L}\right)^{n_2} \tag{5b}$$

where E_1 and $°_1$ are the modulus of elasticity and density at $x = 0$, and E_2 and $°_2$ are the modulus of elasticity and density at $x = L$. n_i is the empirically determined positive inhomogeneity constant . Since the analysis was carried out for a thick wall cylindrical pressure vessel of isotropic FGM, and given that the variation of Poisson's ratio ¬ is small for engineering materials, the Poisson's ratio is assumed to be constant. The stresses on the basis of constitutive equations for non-homogenous and isotropic materials are as follows:

$$\begin{cases} ±_i = ª E\left[(1-¬)£_i + ¬(£_j + £_k)\right], \quad i \ne j \ne k \\ ²_{xz} = ª E\left[(1-2¬)\dfrac{¥_{xz}}{2}\right], \quad ª = \dfrac{1}{(1+¬)(1-2¬)} \end{cases} \tag{6}$$

where $±_i$ and $£_i$ are the stresses and strains in the axial x, circumferential $¯$, and radial z directions. The normal forces (N_x, N_{-}, N_z), shear force (Q_x), bending moments (M_x, M_{-}, M_z), and the torsional moment (M_{xz}) in terms of stress resultants are:

$$\{N_x, N_{-}, N_z\} = \int_{-h/2}^{h/2} \left\{±_x\left(1+\frac{z}{R}\right), ±_{-}, ±_z\left(1+\frac{z}{R}\right)\right\} dz \tag{7a}$$

$$\{M_x, M_{-}, M_z\} = \int_{-h/2}^{h/2} \left\{±_x\left(1+\frac{z}{R}\right), ±_{-}, ±_z\left(1+\frac{z}{R}\right)\right\} z\,dz \tag{7b}$$

$$Q_x = K \int_{-h/2}^{h/2} ²_{xz}\left(1+\frac{z}{R}\right) dz \tag{7c}$$

$$M_{xz} = K \int_{-h/2}^{h/2} ²_{xz}\left(1+\frac{z}{R}\right) z\,dz \tag{7d}$$

where K is the shear correction factor that is embedded in the shear stress term. In the static state, for cylindrical shells $K = 5/6$ [37]. On the basis of the principle of virtual work, the variations of strain energy are equal to the variations of the external work as follows:

$$¢U = ¢W \tag{8}$$

where U is the total strain energy of the elastic body and W is the total external work

due to internal and/or external pressure and centrifugal force. The strain energy is:

$$\begin{cases} U = \iiint_V U^* dV \\ dV = rdrd\theta dx = (R+z)dxd\theta dz \\ U^* = \frac{1}{2}(\sigma_x \varepsilon_x + \sigma_\theta \varepsilon_\theta + \sigma_z \varepsilon_z + \tau_{xz}\gamma_{xz}) \end{cases} \quad (9)$$

The variation of the strain energy is:

$$\delta U = \int_0^{2\pi}\int_0^{L}\int_{-h/2}^{h/2} \delta U^* (R+z) dz dx d\theta \quad (10)$$

The resulting Eq. (11) will be:

$$\frac{\delta U}{2\pi} = \int_0^{L}\int_{-h/2}^{h/2} (\sigma_x \delta\varepsilon_x + \sigma_\theta \delta\varepsilon_\theta + \sigma_z \delta\varepsilon_z + \tau_{xz}\delta\gamma_{xz}) (R+z) dz dx \quad (11)$$

The external work is:

$$W = \iint_S (\vec{f}_{sf} \cdot \vec{u}) dS + \iiint_V (\vec{f}_{bf} \cdot \vec{u}) dV \quad (12)$$

where $\vec{f}_{sf}$ and $\vec{f}_{bf}$ are the body force and the surface force of the rotating pressurized cylinder, respectively. The variation of the external work is as follows:

$$\begin{aligned} \delta W = & \int_0^{2\pi}\int_0^{L} (-P_{in}\delta U_z)\left(R - \frac{h}{2}\right) dx d\theta \\ & + \int_0^{2\pi}\int_0^{L} (-P_{out}\delta U_z)\left(R + \frac{h}{2}\right) dx d\theta \\ & - \int_0^{2\pi}\int_0^{L}\int_{-h/2}^{h/2} \rho\omega^2 (R+z)^2 \delta U_z dz dx d\theta \end{aligned} \quad (13)$$

The resulting Eq. (13) will be:

$$\begin{aligned} \frac{\delta W}{2\pi} = & -\int_0^{L} P_{in}\delta U_z \left(R - \frac{h}{2}\right) dx - \int_0^{L} P_{out}\delta U_z \left(R + \frac{h}{2}\right) dx \\ & - \int_0^{L}\int_{-h/2}^{h/2} \rho\omega^2 (R+z)^2 \delta U_z dz dx \end{aligned} \quad (14)$$

Substituting Eqs. (11) and (14) into Eq. (8), and drawing upon the calculus of variation and the virtual work principle, we will have:

$$\begin{cases} R\dfrac{dN_x}{dx} = 0 \\ R\dfrac{dM_x}{dx} - RQ_x = 0 \\ R\dfrac{dQ_x}{dx} - N_\theta = -P_{in}\left(R - \dfrac{h}{2}\right) - P_{out}\left(R + \dfrac{h}{2}\right) - \dfrac{\rho\omega^2}{6}\dfrac{h}{2}\left(12R^2 + h^2\right) \\ R\dfrac{dM_{xz}}{dx} - M_\theta - RN_z = P_{in}\dfrac{h}{2}\left(R - \dfrac{h}{2}\right) + P_{out}\dfrac{h}{2}\left(R + \dfrac{h}{2}\right) - \dfrac{\rho\omega^2}{6}Rh^3 \end{cases} \quad (15)$$

and the boundary conditions at the two ends of the cylinder are:

$$R\left[N_x \delta u + M_x \delta\theta + Q_x \delta w + M_{xz}\delta\cdot\right]_0^L = 0 \quad (16)$$

In order to solve Eq. (15), forces and moments need to be expressed in terms of the components of displacement field, using Eq. (7). Thus, the set of differential equations could be derived as follows

$$\begin{cases} [\bar{A}_1]\dfrac{d^2}{dx^2}\{\bar{y}\} + [\bar{A}_2]\dfrac{d}{dx}\{\bar{y}\} + [\bar{A}_3]\{\bar{y}\} = \{\bar{F}\} \\ \{\bar{y}\} = \{u \quad \theta \quad w \quad \cdot\}^T \end{cases} \quad (17)$$

Eq. (17) is a set of linear non-homogenous equations with variable coefficients.

$[\bar{A}_3]$ is irreversible and its reverse is needed in the subsequent calculations. In order to make $[\bar{A}_3]^{-1}$, the first equation in the set of Eq. (17) is integrated.

$$RN_x = C_0 \quad (18)$$

In Eq. (17), it is apparent that *u* does not exist, but du/dx does. Taking du/dx as γ,

$$u = \int \gamma dx + C_7 \quad (19)$$

Thus, Eq. (17) could be derived as follows:

$$\begin{cases}[A_1]\dfrac{d^2}{dx^2}\{y\}+[A_2]\dfrac{d}{dx}\{y\}+[A_3]\{y\}=\{F\} \\ \{y\}=\{\text{³} \quad \text{¤} \quad w \quad \cdot\}^T\end{cases} \quad (20)$$

where, the matrices of coefficients $[A_1]_{4\times4}$, and force vector $\{F\}$ are

$$[A_1]=\begin{bmatrix}0 & 0 & 0 & 0\\ 0 & (1-\neg)E\dfrac{Rh^3}{12} & 0 & 0\\ 0 & 0 & \text{«}ERh & \text{«}E\dfrac{h^3}{12}\\ 0 & 0 & \text{«}E\dfrac{h^3}{12} & \text{«}E\dfrac{Rh^3}{12}\end{bmatrix} \quad (21a)$$

$$[A_2]=\begin{bmatrix}0 & (1-\neg)E\dfrac{h^3}{12} & 0 & 0\\ (1-\neg)E\dfrac{h^3}{12} & (1-\neg)\dfrac{dE}{dx}\dfrac{Rh^3}{12} & -\text{«}ERh & -(\text{«}-2\neg)E\dfrac{h^3}{12}\\ 0 & \text{«}ERh & \text{«}\dfrac{dE}{dx}Rh & \text{«}\dfrac{dE}{dx}\dfrac{h^3}{12}\\ 0 & (\text{«}-2\neg)E\dfrac{h^3}{12} & \text{«}\dfrac{dE}{dx}\dfrac{h^3}{12} & \text{«}\dfrac{dE}{dx}\dfrac{Rh^3}{12}\end{bmatrix} \quad (21b)$$

$$[A_3]=\begin{bmatrix}(1-\neg)ERh & 0 & \neg Eh & \neg ERh\\ (1-\neg)\dfrac{dE}{dx}\dfrac{h^3}{12} & -\text{«}ERh & 0 & \neg\dfrac{dE}{dx}\dfrac{h^3}{6}\\ -\neg Eh & \text{«}\dfrac{dE}{dx}Rh & -(1-\neg)E\sim & E\left((1-\neg)R\sim-h\right)\\ -\neg ERh & \text{«}\dfrac{dE}{dx}\dfrac{h^3}{12} & E\left((1-\neg)R\sim-h\right) & -(1-\neg)ER^2\sim\end{bmatrix} \quad (21c)$$

$$\{F\}=\frac{1}{\text{a}}\begin{Bmatrix}C_0\\ 0\\ -P_{in}\left(R-\dfrac{h}{2}\right)-P_{out}\left(R+\dfrac{h}{2}\right)-\dfrac{\text{°}\mu^2}{6}\dfrac{h}{2}\left(12R^2+h^2\right)\\ P_{in}\dfrac{h}{2}\left(R-\dfrac{h}{2}\right)+P_{out}\dfrac{h}{2}\left(R+\dfrac{h}{2}\right)-\dfrac{\text{°}\mu^2}{6}Rh^3\end{Bmatrix} \quad (21d)$$

3. Semi-Analytical Solution

3.1 Multi-layered formulation

Eq. (20) is the set of non-homogenous linear differential equations with variable coefficients. An analytical solution of this set of differential equations with variable coefficients seems to be difficult, if not impossible, to obtain. Hence, in the current study, MLM for the solution of Eq. (20) is presented. In this method, a functionally graded cylinder is divided into homogenous disk layers with constant thickness t . (Fig. 2)

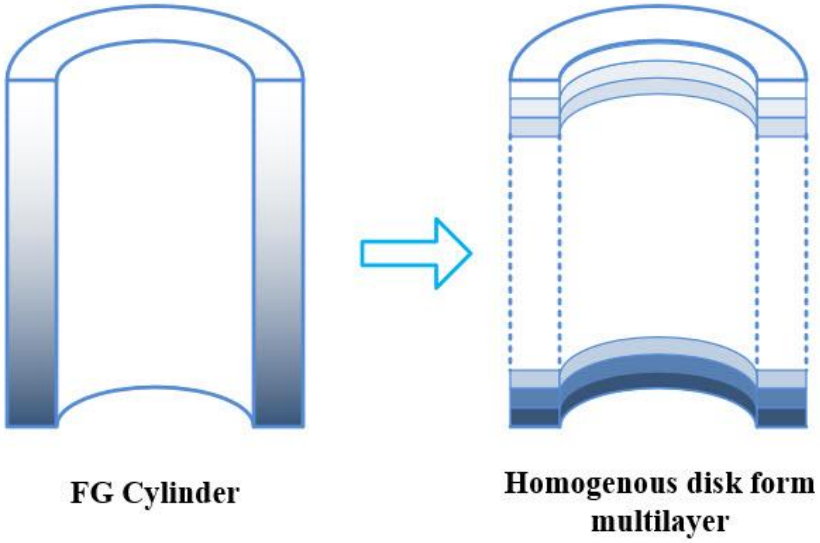

Fig 2. Division of FG cylinder into homogenous disk form multilayer.

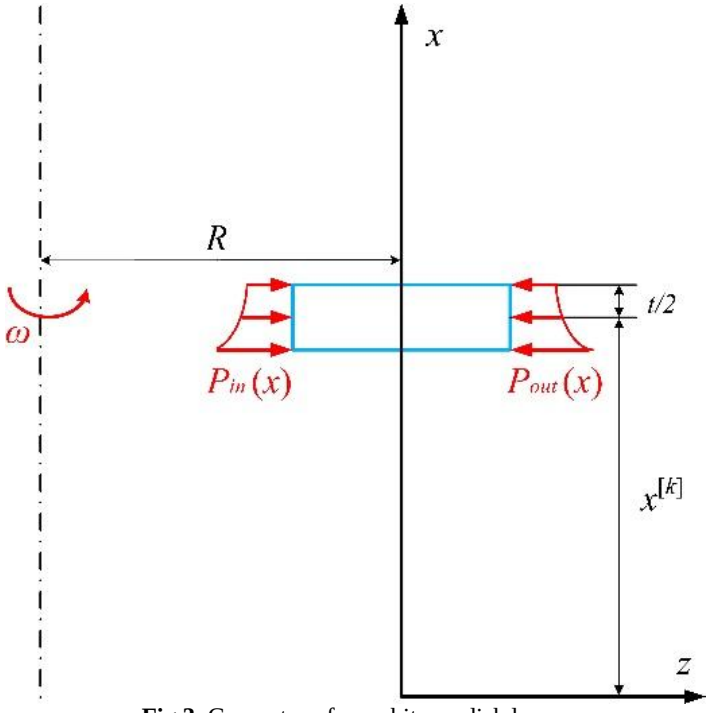

Fig 3. Geometry of an arbitrary disk layer.

Therefore, the governing equations convert to a nonhomogeneous set of differential equations with constant coefficients. $x^{[k]}$ is the length of disks, and n_d is the number of disks. The modulus of elasticity and density of disks are assumed to be constant. The length of middle $x^{[k]}$ of k^{th} disk (Fig. 3) is as follows

$$\left(x^{[k]}-\frac{t}{2}\right)\le x \le\left(x^{[k]}+\frac{t}{2}\right), x^{[k]}=\frac{L}{n}\left(k-\frac{1}{2}\right) \quad (22)$$

The elasticity module and the density of the middle point of each disk are as follows:

$$E^{[k]}=E_1+\left(E_2-E_1\right)\left(\frac{x^{[k]}}{L}\right)^{n_1} \quad (23a)$$

$$\circ^{[k]} = \circ_1 + \left(\circ_2 - \circ_1\right)\left(\frac{x^{[k]}}{L}\right)^{n_2} \qquad (23b)$$

Thus

$$\left(\frac{dE}{dx}\right)^{[k]} = \frac{\left(E_2 - E_1\right)}{Ln_1}\left(\frac{x^{[k]}}{L}\right)^{n_1-1} \qquad (24)$$

With regard to shear stress and based on FSDT, a nonhomogeneous set of differential equations with constant coefficient is obtained for each homogenous disk.

$$\begin{cases} \left[B_1\right]^{[k]}\frac{d^2}{dx^2}\left\{y\right\}^{[k]} + \left[B_2\right]^{[k]}\frac{d}{dx}\left\{y\right\}^{[k]} + \left[B_3\right]^{[k]}\left\{y\right\}^{[k]} = \left\{F\right\}^{[k]} \\ \left\{y\right\}^{[k]} = \left\{\left(du/dx\right)^{[k]} \quad \¤^{[k]} \quad w^{[k]} \quad .^{[k]}\right\}^T \end{cases} \qquad (25)$$

The coefficients matrices $\left[B_i\right]_{4\times4}^{k}$, and force vector $\left\{F\right\}_{4\times1}^{k}$ are as follows:

$$\left[B_1\right]^{[k]} = \begin{bmatrix} 0 & 0 & 0 & 0 \\ 0 & (1-\neg)E^{[k]}\frac{Rh^3}{12} & 0 & 0 \\ 0 & 0 & «E^{[k]}Rh & «E^{[k]}\frac{h^3}{12} \\ 0 & 0 & «E^{[k]}\frac{h^3}{12} & «E^{[k]}\frac{Rh^3}{12} \end{bmatrix} \qquad (26a)$$

$$\left[B_2\right]^{[k]} = \begin{bmatrix} 0 & \left(1-\neg\right)E^{[k]}\frac{h^3}{12} & 0 & 0 \\ \left(1-\neg\right)E^{[k]}\frac{h^3}{12} & \left(1-\neg\right)\left(\frac{dE}{dx}\right)^{[k]}\frac{Rh^3}{12} & -«E^{[k]}Rh & -\left(«-2\neg\right)E^{[k]}\frac{h^3}{12} \\ 0 & «E^{[k]}Rh & «\left(\frac{dE}{dx}\right)^{[k]}Rh & «\left(\frac{dE}{dx}\right)^{[k]}\frac{h^3}{12} \\ 0 & \left(«-2\neg\right)E^{[k]}\frac{h^3}{12} & «\left(\frac{dE}{dx}\right)^{[k]}\frac{h^3}{12} & «\left(\frac{dE}{dx}\right)^{[k]}\frac{Rh^3}{12} \end{bmatrix} \qquad (26b)$$

$$\left[B_3\right]^{[k]} = \begin{bmatrix} \left(1-\neg\right)E^{[k]}Rh & 0 & \neg E^{[k]}h & \neg E^{[k]}Rh \\ \left(1-\neg\right)\frac{dE}{dx}\frac{h^3}{12} & -«E^{[k]}Rh & 0 & \neg\left(\frac{dE}{dx}\right)^{[k]}\frac{h^3}{6} \\ -\neg E^{[k]}h & «\left(\frac{dE}{dx}\right)^{[k]}Rh & -\left(1-\neg\right)E^{[k]}\sim & E^{[k]}\left(\left(1-\neg\right)R\sim - h\right) \\ -\neg E^{[k]}Rh & «\left(\frac{dE}{dx}\right)^{[k]}\frac{h^3}{12} & E^{[k]}\left(\left(1-\neg\right)R\sim - h\right) & -\left(1-\neg\right)E^{[k]}R^2\sim \end{bmatrix} \qquad (26c)$$

$$\{F\}^{[k]}=\begin{Bmatrix} C_0 \\ 0 \\ -P_{in}\left(R-\frac{h}{2}\right)-P_{out}\left(R+\frac{h}{2}\right)-\frac{\rho^{[k]}\omega^2}{6}\frac{h}{2}\left(12R^2+h^2\right) \\ P_{in}\frac{h}{2}\left(R-\frac{h}{2}\right)+P_{out}\frac{h}{2}\left(R+\frac{h}{2}\right)-\frac{\rho^{[k]}\omega^2}{6}Rh^3 \end{Bmatrix} \quad (26d)$$

3.2 Elastic Solution

Defining the differential operator $P(D)$, Eq. (26) is written as

$$\begin{cases} [P(D)]^{[k]}=[B_1]^{[k]}D^2+[B_2]^{[k]}D+[B_3]^{[k]} \\ D^2=\frac{d^2}{dx^2}, D=\frac{d}{dx} \end{cases} \quad (27)$$

Thus

$$[P(D)]^{[k]}\{y\}^{[k]}=\{F\}^{[k]} \quad (28)$$

The differential equations given above have the total solution including the general solution for the homogeneous case and the particular solution, as follows:

$$\{y\}^{[k]}=\{y\}_h^{[k]}+\{y\}_p^{[k]} \quad (29)$$

For the homogeneous case,

$$\begin{cases} [P(D)]^{[k]}\{y\}_h^{[k]}=0 \\ \{y\}_h^{[k]}=\{V\}^{[k]}e^{m^{[k]}x} \end{cases} \quad (30)$$

With respect to Eq. (27), we have:

$$\left|m^2[B_1]^{[k]}+m[B_2]^{[k]}+[B_3]^{[k]}\right|=0 \quad (31)$$

The result of the determinant above is a six-order polynomial, which is a function of m, the solution of which is a 6-eigenvalue m_i. The eigenvalues are 3 pairs of conjugated roots. Substituting the calculated eigenvalues in the following equation, the corresponding eigenvectors are obtained.

$$\left[m^2[B_1]^{[k]}+m[B_2]^{[k]}+[B_3]^{[k]}\right]\{V\}^{[k]}=0 \quad (32)$$

Therefore, the homogeneous solution is

$$\{y\}_h^{[k]}=\sum_{i=1}^{6}C_i^{[k]}\{V\}_i^{[k]}e^{m_i^{[k]}x} \quad (33)$$

The particular solution is obtained as follows.

$$\{y\}_p^{[k]}=\left[[B_3]^{[k]}\right]^{-1}\{F\}^{[k]} \quad (34)$$

Therefore, the total solution is

$$\{y\}^{[k]}=\sum_{i=1}^{6}C_i\{V\}_i^{[k]}e^{m_i^{[k]}x}+\left[[B_3]^{[k]}\right]^{-1}\{F\}^{[k]} \quad (35)$$

In general, the problem for each disk consists of 8 unknown values of C_i, including C_0 (Eq. (18)), C_1 to C_6 (Eq. (35)), and C_7 (Eq. (36))

$$u^{[k]}=\int\left(du/dx\right)^{[k]}dx+C_7 \quad (36)$$

The elastic solution is completed by the application of the boundary and continuity conditions.

3.3 Boundary and Continuity Conditions

Using SDT, it could be assumed that the cylinder has boundary conditions other than free–free ends. The clamped–clamped (fixed–fixed) boundary is straightforward and implies that the ends of the cylinder are restrained in all coordinate directions and even with that the plane along the edge of the cross-section is assumed not to rotate as opposed to a line tangent to the mid-surface of the shell as in thin shell theories. Simple support end conditions can be given a variety of interpretations [38]. Classically, a simple support boundary condition is characterized with a hinge (ball and socket in three dimensions) or roller if motion is not restrained in all directions. In Table 1 the details of boundary condition for the rotating cylindrical shell are presented.

Table 1. Boundary conditions for each end of cylindrical shell

	Direction	Clamped supported	Simply supported	Free end
Boundary condition	x	$u=0$	$u=0$	$N_x=0$
		¤ $=0$	$M_x=0$	$M_x=0$
	z	$w=0$	$w=0$	$Q_x=0$
		· $=0$	$M_{xz}=0$	$M_{xz}=0$

In this work, two end edges of the FGM cylindrical shells are assumed to be clamped supported. Because of continuity and homogeneity of the cylinder, at the boundary between the two layers, forces, stresses and displacements must be continuous. Given that SDT applied is an approximation of one order and also all equations related to the stresses include the first derivatives of displacement, the continuity conditions are as follows:

$$\left\{\begin{matrix} U_x^{[k-1]}(x,z) \\ U_z^{[k-1]}(x,z) \end{matrix}\right\}_{x=x^{[k-1]}+\frac{t}{2}} = \left\{\begin{matrix} U_x^{[k]}(x,z) \\ U_z^{[k]}(x,z) \end{matrix}\right\}_{x=x^{[k]}-\frac{t}{2}} \quad (37)$$

$$\left\{\begin{matrix} U_x^{[k]}(x,z) \\ U_z^{[k]}(x,z) \end{matrix}\right\}_{x=x^{[k]}+\frac{t}{2}} = \left\{\begin{matrix} U_x^{[k+1]}(x,z) \\ U_z^{[k+1]}(x,z) \end{matrix}\right\}_{x=x^{[k+1]}-\frac{t}{2}} \quad (38)$$

And

$$\left\{\begin{matrix} \frac{dU_x^{[k-1]}(x,z)}{dx} \\ \frac{dU_z^{[k-1]}(x,z)}{dx} \end{matrix}\right\}_{x=x^{[k-1]}+\frac{t}{2}} = \left\{\begin{matrix} \frac{dU_x^{[k]}(x,z)}{dx} \\ \frac{dU_z^{[k]}(x,z)}{dx} \end{matrix}\right\}_{x=x^{[k]}-\frac{t}{2}} \quad (39)$$

$$\left\{\begin{matrix} \frac{dU_x^{[k]}(x,z)}{dx} \\ \frac{dU_z^{[k]}(x,z)}{dx} \end{matrix}\right\}_{x=x^{[k]}+\frac{t}{2}} = \left\{\begin{matrix} \frac{dU_x^{[k+1]}(x,z)}{dx} \\ \frac{dU_z^{[k+1]}(x,z)}{dx} \end{matrix}\right\}_{x=x^{[k+1]}-\frac{t}{2}} \quad (40)$$

Given the continuity conditions, in terms of z, 8 Equations are obtained. In general, if the cylinder is divided into n disk layers, $8(n_d-1)$ equations are obtained. Using the 8 equations of the boundary condition, $8n_d$ equations are obtained. The solution of these equations yields $8n_d$ unknown constants.

4. Results and Discussion

In this section, numerical calculations are carried out for specific cases. In order to show the effectiveness and accuracy of the approach suggested here, a comparison between responses of the present theories and FEM can be made. In FEM, an FG cylinder was modeled using ANSYS®. The PLANE 223 element in axisymmetric mode, which is an element with eight nodes with up to four degrees of freedom per each node, was used for discretization. In order to model axially FG cylinder, an innovative application for multi-layering of thickness in the axial direction has been performed. Homogenous layers which are of identical thickness and step-variable properties have been formed by this method. Using 6 elements in radial coordinate and 210 elements in axial coordinate (1260 elements), finite element analysis was carried out to obtain the benchmark solution.

A cylindrical shell with $r_i = 40$ mm, $h = 20$ mm and $L = 800$ mm is considered in this paper. The thick cylindrical has clamped-clamped boundary conditions. For axial distribution of pressure, the model of Eq. (41) is selected:

$$P_{in}(x) = P_1 + (P_2 - P_1)\left(\frac{x}{L}\right)^m, P_{out}(x) = 0 \quad (41)$$

Here P_1 and P_2 are the values of internal pressure at the $x=0$ and $x=L$, respectively. m is constant parameter that is used to control the pressure profile. In order to compute the numerical results, the following material properties and boundary conditions are used for each end of the cylinder. (Table 2)

Table 2. Material properties and boundary conditions for each end of cylinder

	E (GPa)	° (kg/m^3)	¬	P (MPa)	µ (rad/s)
$x=0$	200	7800	0.3	120	1000
$x=L$	70	3000	0.3	40	1000

The results are presented in a non-dimensional form. Displacement was normalized by dividing to the internal radii. In order to normalize stresses, we define the mean internal pressure parameter as follows:

$$\bar{P}=\frac{P_1+P_2}{2} \tag{42}$$

The effect of the number of disk layers on the radial displacement is shown in Fig. 4. It could be observed that if the number of disk layers is fewer than 80, it will have a significant effect on the response. However, if the number of layers is more than 80 disks, there will be no significant effect on radial displacement. In the problem in question 100 disks are used.

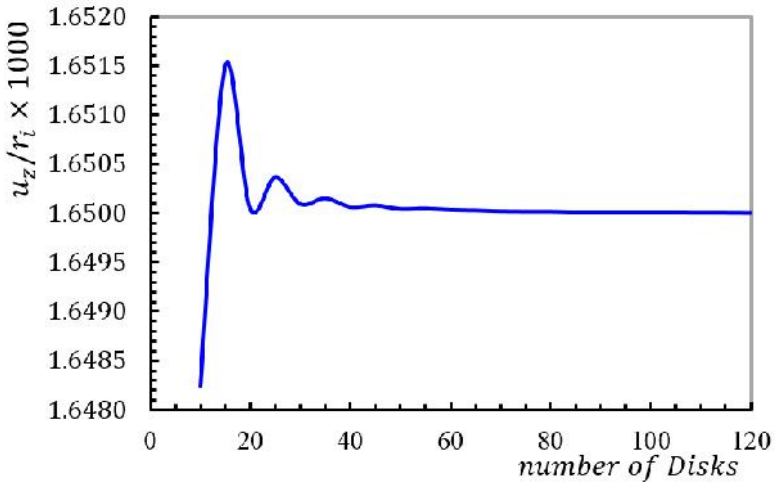

Fig 4. Effect of the number of disk layers on the normalized radial displacement $(m=2, n=1.5)$.

In Figs. 5 to 8, displacement and stress distributions are obtained, using MLM, are compared with the solutions of FEM and are presented in the form of graphs. Figs. 5-8 show that the disk layer method based on FSDT has an acceptable amount of accuracy when one wants to obtain radial displacement, radial stress, circumferential stress and shear stress.

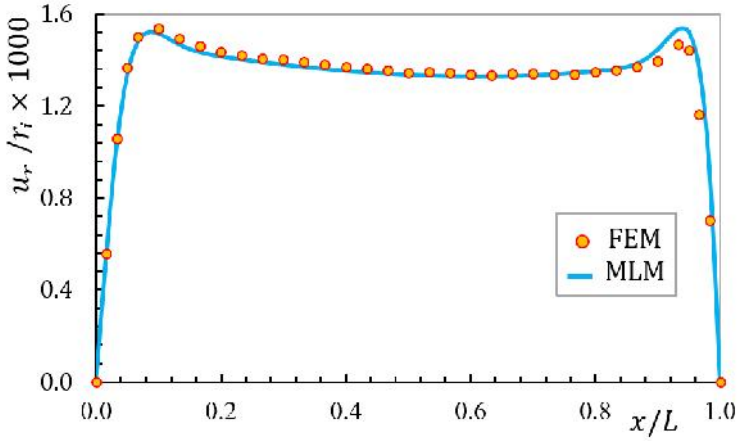

Fig 5. Normalized radial displacement distribution in middle layer $(m=1, n=1.5)$.

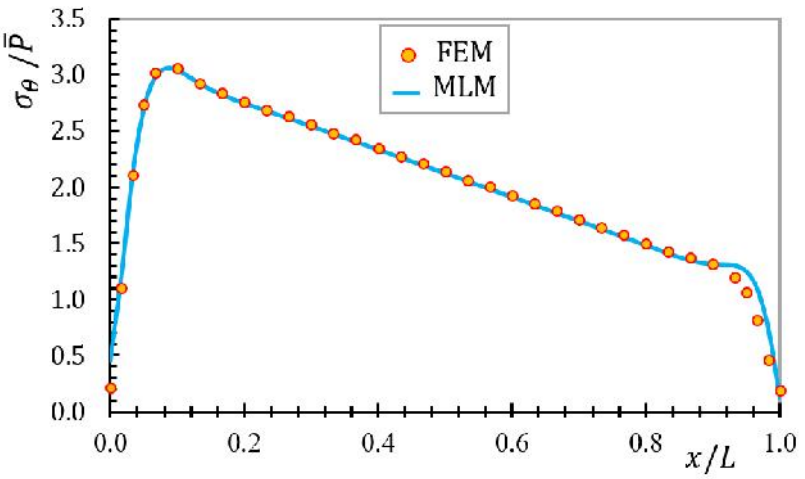

Fig 6. Normalized circumferential stress distribution in middle layer $(m=1, n=1.5)$.

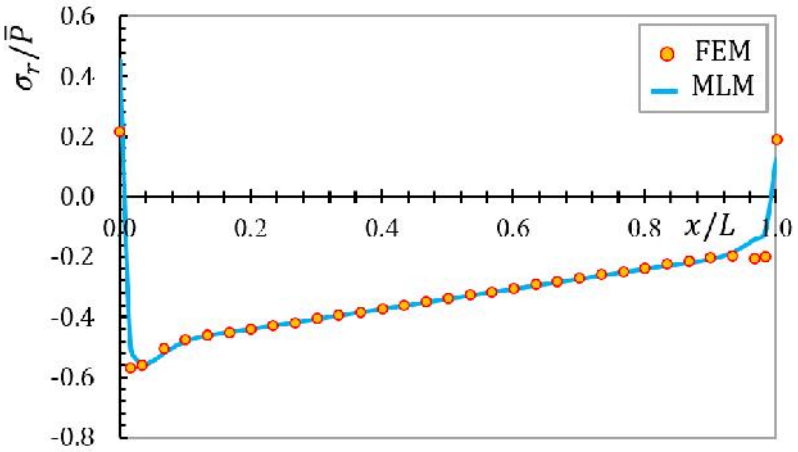

Fig 7. Normalized radial stress distribution in middle layer $(m=1, n=1.5)$.

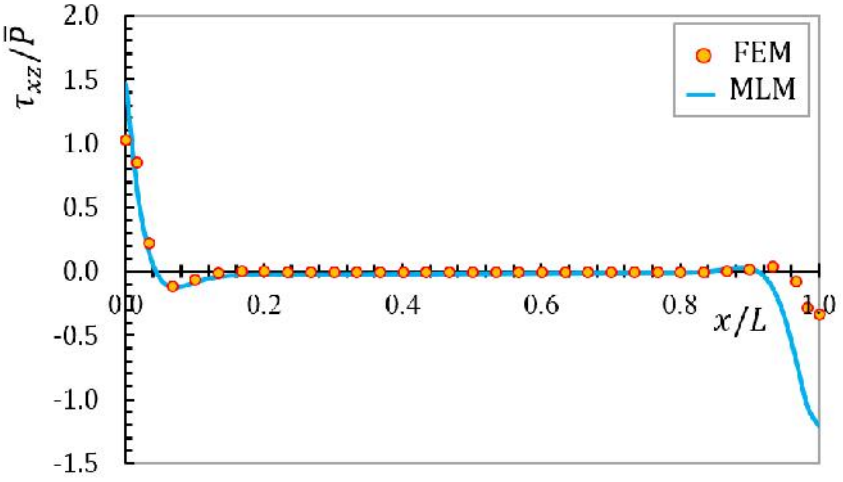

Fig 8. Normalized shear stress distribution in middle layer $(m=1, n=1.5)$.

The effects of angular velocity ω on the distribution of the stresses and radial displacement are presented in Figs. 9 and 10. Figs. 9 and 10 indicate that radial displacement and equivalent stress rise with increase in angular velocity. Also for the angular speed less than 500 rad/s, the centrifugal force is less effective than the internal pressure. It can be noted that at very near the axial boundaries of the cylinder, the mechanical response shows a different characteristic from its general behavior over the maximum part of the cylinder. In this very small region, due to edge moments subjected to clamped-clamped boundary condition, the absolute value of radial displacement and von-Mises stress have a higher value from the points away from boundaries. The results of FG rotating cylinder are presented to study the impact of the non-uniformity pressure function on the results. For this purpose, the distribution of pressure for different values of m could be seen in Fig. 11. Fig. 11 shows that a linear pressure distribution can be obtained by setting $m=1$. The pressure profile is concave if $m<1$ and it is convex if $m>1$. Figs. 11 and 12 indicate that radial displacement and equivalent stress rise with increase in non-uniformity pressure constant m.

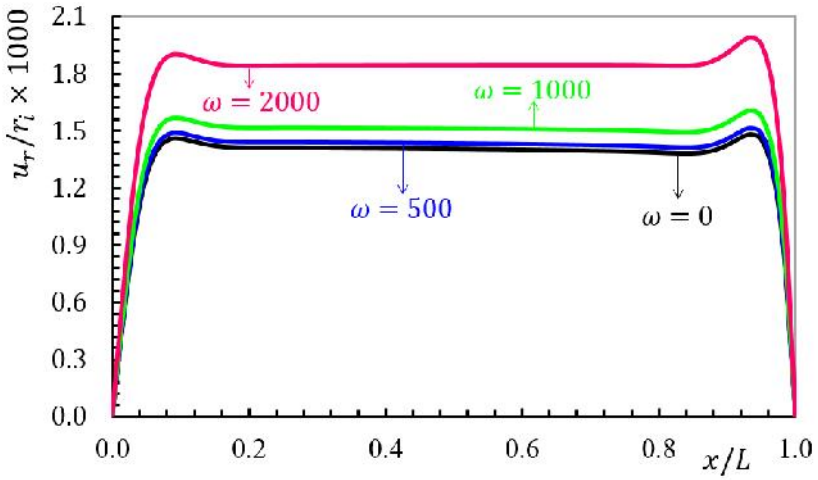

Fig 9. Normalized radial displacement subjected to various angular velocity $(m=1, n=1)$.

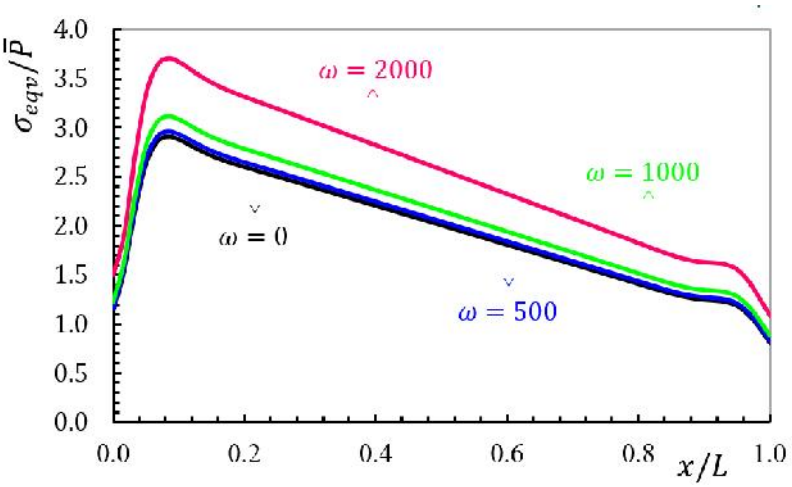

Fig 10. Normalized von Mises stress subjected to various angular velocity $(m=1, n=1)$.

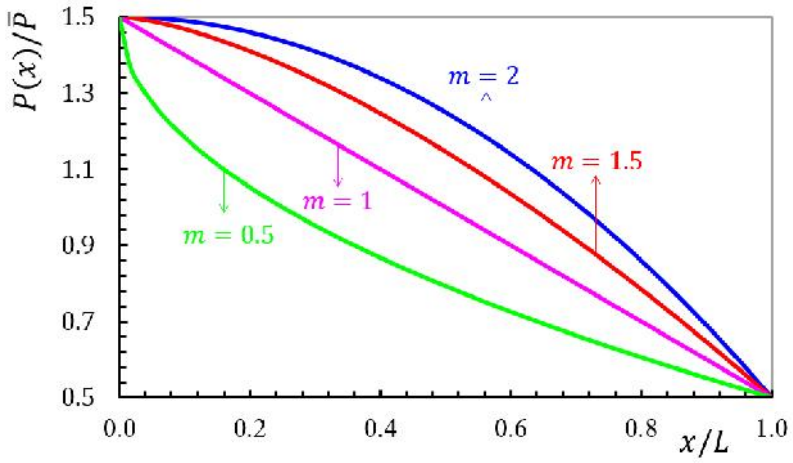

Fig 11. Axial distribution of non-dimensional inner pressure.

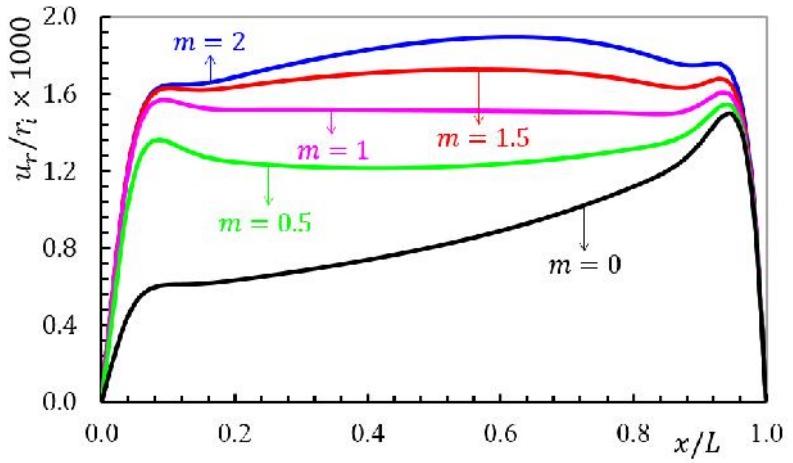

Fig 12. Normalized radial displacement along the length subjected to different internal pressure profiles $(n = 1)$.

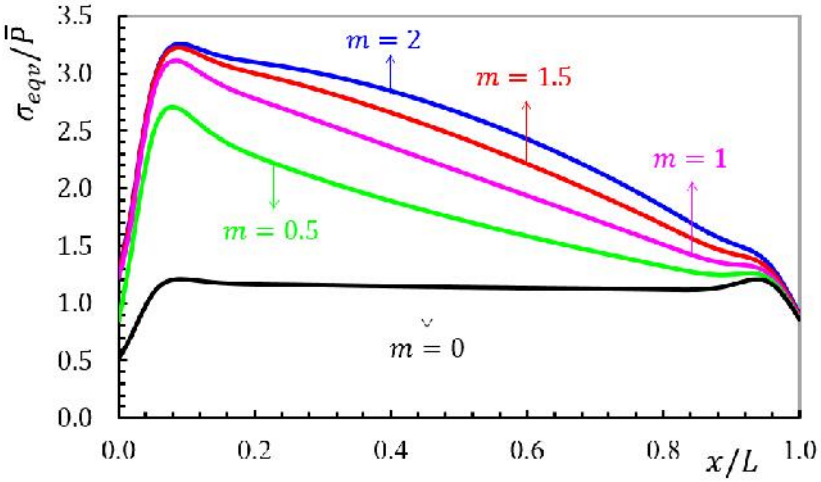

Fig 13. Normalized von Mises stress along the length subjected to different internal pressure profiles $(n = 1)$.

The radial distribution of modulus of elasticity is showed in Fig. 14. It is obvious that in the same position $(0 < x/L < 1)$, the dimensionless modulus of elasticity decreases as n decreases. Also, due to the similarity between density and elasticity modulus, the density distribution curve is similar to Fig. 14.

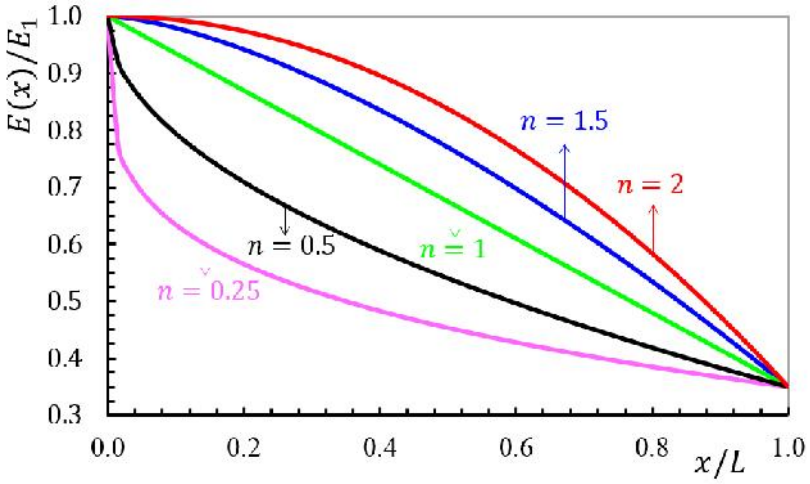

Fig 14. Non-dimensional modulus of elasticity along the length for different non-homogeneity indexes.

The influences of gradient index on the distribution of displacement and equivalent stress are examined in Figs. 15 and 16. The results of Figs. 15 and 16 can be summarized to conclude that in the FG cylinder with axially-varying properties according to Power-law form, higher gradient index is better than lower gradient index. It could be observed that the radial displacement decreases with the increase in the grading index n from zero up to its maximum value $n \to \infty$. Also, it is observed that the choice of power-law index is entirely dependent on the pressure function. For example, in the case of $m = 1$ (linear pressure function) and $n = 1$ (linear gradient properties), radial displacement is constant for distant points of the boundaries.

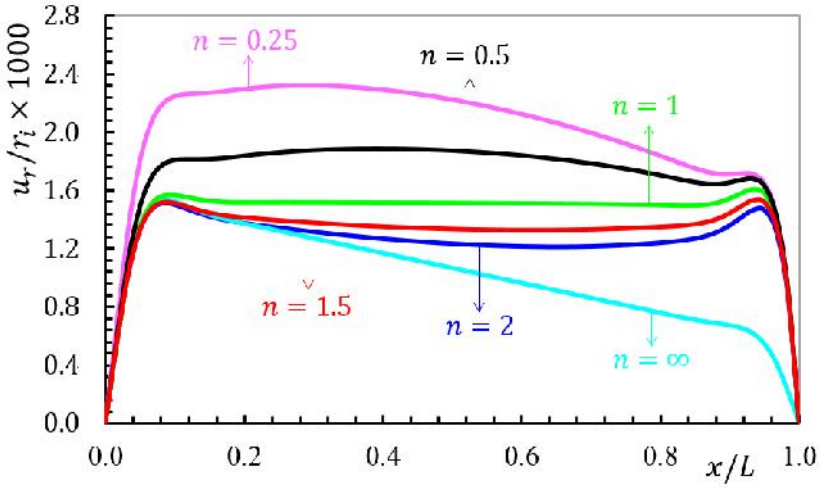

Fig 15. Normalized radial displacement subjected to different non-homogeneity indexes $(m = 1)$.

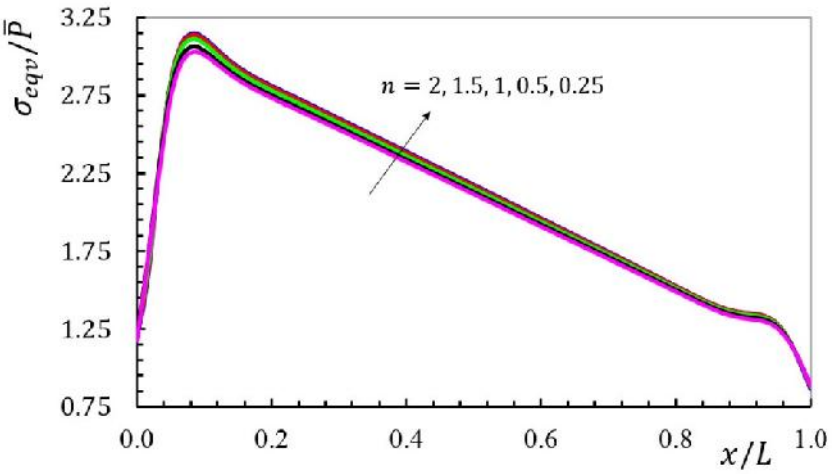

Fig 16. Normalized von Mises stress subjected to different non-homogeneity indexes $(m = 1)$.

5. Conclusions

In the present study, based on FSDT and elasticity theory, the governing equations of thick-walled cylindrical shell are derived. The mechanical properties except Poisson ratio, are graded along the axial direction according to a power law form of axial direction. A thick FG cylindrical shell is divided into homogenous disks with constant height. With regard to the continuity between layers and applying boundary conditions, the governing set of differential equations with constant coefficients is solved. The results obtained for stresses and displacements are compared with the solutions carried out through the FEM. Good agreement was found between the results. General observations of this study could be summarized as follows:

1. SDT is a popular model in structural analysis. In SDT, any changes in the axial direction of a cylindrical shell cause variable coefficients in the governing differential equations. The system of differential equations with variable coefficients can be changed to a set of differential equations with constant coefficients by MLM method.
2. The results show that MLM, based on FSDT, has an acceptable amount of accuracy when one wants to obtain radial displacement, radial stress, circumferential stress and shear stress.
3. By using axially FG cylinder, radial displacement can be uniform in the axial direction under non-uniform pressure.
4. For the angular speed less than 500 rad/s, the centrifugal force effect is negligible.

References

[1] M. Z. Nejad, M. Gharibi, “Effect of material gradient on stresses of thick FGM spherical pressure vessels with exponentially-varying properties”, J. Adv. Mat. and Proc., Vol. 2, no. 3, 2014, pp. 39-46.

[2] M. Z. Nejad, M. Jabbari, M. Ghannad, “Elastic analysis of FGM rotating thick truncated conical shells with axially-varying properties under non-uniform pressure loading”, Compos. Struct., Vol. 122, 2015, pp. 561-569.

[3] H. L. Dai, Y. N. Rao, “Dynamic thermoelastic behavior of a double-layered hollow cylinder with an FGM layer”, J. Therm. Stresses, Vol. 36, no. 9, 2013, pp. 962-984.

[4] M. Z. Nejad, M. Jabbari, M. Ghannad, “Elastic analysis of axially functionally graded rotating thick cylinder with variable thickness under non-uniform arbitrarily pressure loading”, Int. J. Eng. Sci., Vol. 89, 2015, pp. 86-99.

[5] M. Jabbari, M. Z. Nejad, M. Ghannad, “Thermo-elastic analysis of axially functionally graded rotating thick cylindrical pressure vessels with variable thickness under mechanical loading”, Int. J. Eng. Sci., Vol. 96, 2015, pp. 1–18.

[6] G. Lamé, B. Clapeyron, “Mémoire sur l'équilibre intérieur des corps solides

homogènes", Journal für die reine und angewandte Mathematik, 1831, pp. 145-169.
[7] P. M. Naghdi, R. M. Cooper, "Propagation of elastic waves in cylindrical shells, including the effects of transverse shear and rotatory inertia", J. Acous. Soc. America, Vol. 28, no. 1, 1956, pp. 56-63.
[8] I. Mirsky, G. Hermann, "Axially motions of thick cylindrical shells", J. Appl. Mech., Vol. 25, 1958, pp. 97-102.
[9] F. Erdogan, G. Gupta, "The stress analysis of multi-layered composites with a flaw",, Int. J. Solids Struct., Vol. 7, no. 1, 1971, pp. 39-61
[10] K. Shirakawa, "Displacements and stresses in cylindrical shells based on an improved theory", Int. J. Mech. Sci., Vol. 26, no. 2, 1984, pp. 93-103.
[11] J. N. Reddy, "A refined nonlinear theory of plates with transverse shear deformation",, Int. J. Solids Struct., Vol. 20, no. 9/10, 1984, pp. 881-896
[12] C. O. Horgan, A. M. Chan, "The pressurized hollow cylinder or disk problem for functionally graded isotropic linearly elastic materials", J. Elast., Vol. 55, no. 1, 1999, pp. 43-59.
[13] F. I. Niordson, "An asymptotic theory for circular cylindrical shells", Int. J. Solids Struct., Vol. 37, no. 13, 2000, pp. 1817-1839.
[14] T. Y. Ng, K. Y. Lam, K. M. Liew, J. N. Reddy, "Dynamic stability analysis of functionally graded cylindrical shells under periodic axial loading", Int. J. Solids Struct., Vol. 38, no. 8, 2001, pp. 1295–1309.
[15] E. Pan, A. K. Roy, "A simple plane-strain solution for functionally graded multilayered isotropic cylinders", Struc. Eng. Mech., Vol. 24, no. 6, 2006, pp. 727-740.
[16] H. Xiang, Z. Shi, T. Zhang, "Elastic analyses of heterogeneous hollow cylinders", Mech. Res. Commun., Vol. 33, no. 5, 2006, pp. 681-691.
[17] J. H. Kang, "Field equations, equations of motion, and energy functionals for thick shells of reVolution with arbitrary curvature and variable thickness from a three-dimensional theory", Acta Mech., Vol. 188, no. 1-2, 2007, pp. 21-37.
[18] M. Z. Nejad, G. H. Rahimi, M. Ghannad, "Set of field equations for thick shell of revolution made of functionally graded materials in curvilinear coordinate system", Mechanika, Vol. 77, no. 3, 2009, pp. 18-26.
[19] H. Santos, C. M. M. Soares, C. A. M. Soares, J. N. Reddy, "A semi-analytical finite element model for the analysis of cylindrical shells made of functionally graded materials", Compos. Struct., Vol. 91, no. 4, 2009, pp. 427-432.
[20] N. Tutuncu, B. Temel, "A novel approach to stress analysis of pressurized FGM cylinders, disks and spheres", Compos. Struct., Vol. 91, no. 3, 2009, pp. 385-390.
[21] M. Z. Nejad, G. H. Rahimi, "Elastic analysis of FGM rotating cylindrical pressure vessels", J. Chin. Ins. Eng., Vol. 33, no. 4, 2010, pp. 525-530.
[22] A. G. Arani, Z. K., M. R. M. Maraghi, A. R. Shajari, "Thermo-piezo-magneto-mechanical stresses analysis of FGPM hollow rotating thin disk", Int. J. Mech. Mater. Des., Vol. 6, 2011, pp. 341-349,
[23] M. Ghannad, M. Z. Nejad, "Complete elastic solution of pressurized thick cylindrical shells made of heterogeneous functionally graded materials", Mechanika, Vol. 18, no. 6, 2012, pp. 640-649.
[24] V. V. Zozulya, "A high-order theory for functionally graded axially symmetric cylindrical shells", Arc. App. Mech., Vol. 83, no. 3, 2013, pp. 331-343.
[25] M. Ghannad, M. Z. Nejad, "Elastic analysis of pressurized thick hollow cylindrical shells with clamped-clamped ends", Mechanika, Vol. 5, no. 85, 2010, pp. 11-18.
[26] M. Ghannad, M. Z. Nejad, "Elastic solution of pressurized clamped-clamped thick cylindrical shells made of functionally graded materials", J. Theor. App. Mech., Vol. 51, no. 4, 2013, pp. 1067-1079.
[27] M. Ghannad, H. Gharooni, "Displacements and stresses in pressurized thick FGM cylinders with varying properties of power function based on HSDT", J. Sol. Mech., Vol. 4, no. 3, 2012, pp. 237-251.
[28] M. J. Khoshgoftar, G. H. Rahimi, M. Arefi, "Exact solution of functionally graded thick cylinder with finite length under longitudinally non-uniform pressure", Mech. Res. Commun., Vol. 51, 2013, pp. 61-66.
[29] M. Ghannad, G. H. Rahimi, M. Z. Nejad, "Determination of displacements and stresses in pressurized thick cylindrical shells

with variable thickness using perturbation technique", Mechanika, Vol. 18, no. 1, 2012, pp. 14-21.

[30] M. Ghannad, G. H. Rahimi, M. Z. Nejad, "Elastic analysis of pressurized thick cylindrical shells with variable thickness made of functionally graded materials", Comp. Part B- Eng., Vol. 45, no. 1, 2013, pp. 388-396.

[31] K. Asemi, M. Salehi, M. Akhlaghi, "Elastic solution of a two-dimensional functionally graded thick truncated cone with finite length under hydrostatic combined loads", Acta Mech., Vol. 217, no. 1-2, 2011, pp. 119-134.

[32] M. Z. Nejad, M. Jabbari, M. Ghannad, "A semi-analytical solution for elastic analysis of rotating thick cylindrical shells with variable thickness using disk form multilayers", Sci. Wor. J., 2014, Article ID, 932743, pp. 1-10.

[33] A. G. Arani, E. Haghparast, Z. K. Maraghi, S. Amir, "Static stress analysis of carbon nano-tube reinforced composite (CNTRC) cylinder under non-axisymmetric thermo-mechanical loads and uniform electro-magnetic fields", Comp. Part B- Eng., Vol. 68, 2014,136-145.

[34] R. C. Batra, "Material tailoring in finite torsional deformations of axially graded Mooney–Rivlin circular cylinder", Math. Mech. Sol., Vol. 20, no. 2, 2015, pp. 183-189.

[35] M. Z. Nejad, M. Jabbari, M. Ghannad, "Elastic analysis of rotating thick cylindrical pressure vessels under non-uniform pressure: linear and non-linear thickness", Periodica Poly. Mech.Eng., Vol. 59, no. 2, 2015, pp. 5-73.

[36] M. Shariati, H. Sadeghi, M. Ghannad, H. Gharooni, "Semi analytical analysis of FGM thick-walled cylindrical pressure vessel with longitudinal variation of elastic modulus under internal pressure", J. Sol. Mech., Vol. 7, no. 2, 2015, pp. 131-145.

[37] S. Vlachoutsis, "Shear correction factors for plates and shells", Int. J. Numer. Methods Eng., Vol. 33, 1992, pp. 1537–1552.

[38] G. R. Buchanan, C. B. Y. Yii, "Effect of symmetrical boundary conditions on the vibration of thick hollow cylinders", App. Acou., Vol. 63, no. 5, 2002, pp. 547-566.